The 2010 IEEE/RSJ International Conference on
Intelligent Robots and Systems
October 18-22, 2010, Taipei, Taiwan

A Sensor Platform for Outdoor Navigation Using Gyro-assisted Odometry and Roundly-swinging 3D Laser Scanner

Tomoaki Yoshida, Kiyoshi Irie, Eiji Koyanagi and Masahiro Tomono

Abstract— **This paper proposes a light-weight sensor platform that consists of gyro-assisted odometry and a 3D laser scanner for localization of human-scale robots. The gyro-assisted odometry provides highly accurate positioning only by dead-reckoning. The 3D laser scanner has a wide field of view and uniform measuring-point distribution. Robust and computationally inexpensive localization is implemented on the sensor platform using a particle filter on a 2D grid map generated by projecting 3D points on to the ground. The system uses small and low-cost sensors, and can be applied to a variety of mobile robots in human-scale environments. Outdoor navigation experiments were performed at the Tsukuba Challenge 2009, which is an open proving ground for human-scale robots. Our robot successfully navigated the assigned 1-km course in a fully autonomous mode multiple times.**

I. INTRODUCTION

Mobile service robots that move around in human living spaces have many promising applications such as transporting, guiding, security and cleaning [1], [2], [3]. These robots are required to navigate outdoor as well as indoor environments, and robust outdoor navigation is an important issue to develop them. There have been many studies on outdoor navigation for autonomous mobile robots, including the Grand Challenge and Urban Challenge [4]. The scale of the target environments for these studies is relatively large because they aim to develop car-like robots that can navigate through driveways. On the other hand, the abovementioned service robots are relatively small and lightweight to navigate in human living spaces such as narrow passageways, open spaces, passages near buildings or trees, and even entering buildings. In such environments where radio signals are occluded and reflected, the positioning obtained from GPS will be unstable. Moreover, due to the limited size of human-scale robots, only a small number of sensors and computers can be mounted on them.

One of the main difficulties of outdoor navigation is the self-localization of robots under various conditions. In indoor environments, walls and furniture can be used as valuable landmarks. However, in outdoor environments, there are often many open spaces and very few landmarks. Hence, a more precise and robust navigation system is required for outdoor environments. Dead-reckoning and star-reckoning are well-known techniques for achieving robot localization. Dead-reckoning accumulates errors and cannot be used for navigating long distances. Star-reckoning needs to observe landmarks in the environment and cannot be utilized without any landmark observations. One important approach to these problems is sensor fusion. Probabilistic frameworks that combine these two methods using Kalman filters and particle filters have been proposed to achieve high precision and robustness[5], [6]. Another important approach is to improve sensor performance; inertial sensors with less accumulated errors for accurate dead-reckoning and external sensors with a wide-view angle for observing more landmarks.

Odometry is usually used for dead-reckoning in wheeled mobile robots by measuring the rotational speed of two wheels using encoders. Odometry has accumulated errors, in which orientation errors have a large impact on the precision of the estimated position. An approach to this problem is to measure the rotational motion with a gyroscope. However, gyroscopes also accumulate errors due to factors such as offset drift, and a simple combination with odometry may not reduce the positioning errors. There have been many solutions proposed to solve this problem, such as a sensor fusion method using Extended Kalman Filter(EKF) [7], adaptively switching a sensor for rotational motion between the gyroscope and encoders [8], filter out gyro drift using heuristics[9], etc. These method depends on a precise error model or a specific use case.

2D laser scanners are popular external sensors for mobile robots because they have a good performance balance in terms of sensing speed, precision and cost. In indoor environments, there are walls and furniture whose locations can easily be detected and used as landmarks by horizontally placed scanners. Outdoor environment often have fewer or no structured landmarks such as walls or buildings, and the number of landmarks detected by a single horizontal scanner may not be sufficient. To cope with this problem, laser scanners that can nod or rotate to extend their field of view are frequently employed. Both nodding and rotating method has singularities of the point distribution. In addition, the rotating method needs special cable handling for the embedded 2D laser scanner, and the nodding method needs reciprocal motion.

This paper proposes a sensor platform for mobile robots that integrates a gyro-assisted high-precision odometry and a wide-view roundly-swinging three-dimensional (3D) laser scanner. The gyro-assisted high-precision odometry consists of two complementary gyroscopes attached to the same yaw axis to compensate each other's drift. The roundly-swinging 3D scanner consists of a 2D laser scanner attached to a gimbal and a single actuator. It has uniformly distributed measuring points in a wide angle of view. Robust self-localization is implemented on the sensor platform with a

All authors are with Future Robotics Technology Center, Chiba Institute of Technology, 2-17-1 Tsudanuma, Narashino-shi, Chiba , Japan {irie, yoshida, tomono, koyanagi}@furo.org

particle filter to fuse the measurements from the gyro-assisted odometry and the 3D laser scanner. The likelihood computation in the particle filter is based on map-matching using a 2D grid map which is generated by projecting 3D points on to the ground. This makes the particle filter computationally inexpensive while maintaining the rich information from the wide angle of view. The system is built using small and low-cost sensors, and it can be applied to a wide variety of mobile robots for human-scale environments.

We performed experiments on outdoor navigation at the Tsukuba Challenge [10], which is an open proving ground for human-scale robots. The reliability of the proposed system was verified by the experimental results, which showed that the robot successfully navigated the assigned 1-km course in a fully autonomous mode multiple times.

II. Gyro-assisted high-precision odometry

A. Sources of positioning errors

Odometers calculate the longitudinal and rotational motions by measuring the rotational speed of two wheels using encoders. The accumulated errors of odometry are affected by systematic errors, such as inaccurate parameters for the wheel diameter and tread width, and non-systematic errors, such as wheel slippage or bumps on the floor. In particular, orientation errors have a large impact on the precision of the estimated position. By using gyroscopes to measure the rotational speed directly, both systematic and non-systematic errors can be avoided to improve the positioning accuracy. However, gyroscopes also accumulate orientation errors due to such factors as drift, rounding errors, etc.

We use the MEMS rate gyro CRS-10 (Silicon Sensing) to measure the rotational speed for odometry calculation.

The following factors are major error sources when calculating orientations using MEMS rate gyros.

- Drifting offset caused by temperature change
- Analog noise from power supply or other electrical components
- Rounding errors from ADC and computation process

The drifting offset value is relatively larger for MEMS rate gyros than fiber optic gyros. The amount of rounding errors is determined by the ADC resolution and the dynamic range of gyro output. In implementation, we used gyros configured to a rate of 75[°/s] and full-scale analog range of ± 2.07[V], attached to a 12-bit ADC with V_{ref} = 5[V]. As a result, 1 LSB is equivalent to 0.044 [°/s].

B. Reduction of orientation errors

To compensate for the offset drift caused by temperature change, each time a robot stops moving, the gyro output is measured to calibrate the offset values. The stationary condition is detected by monitoring the encoder output on both wheels, and when the same value is recorded for over 1 [s], the offset value is updated with the weighted mean using the old value and averaged gyro output in the meantime. In addition, using two complementary gyros attached to the same yaw axis and providing two outputs helps cancel the offset errors.

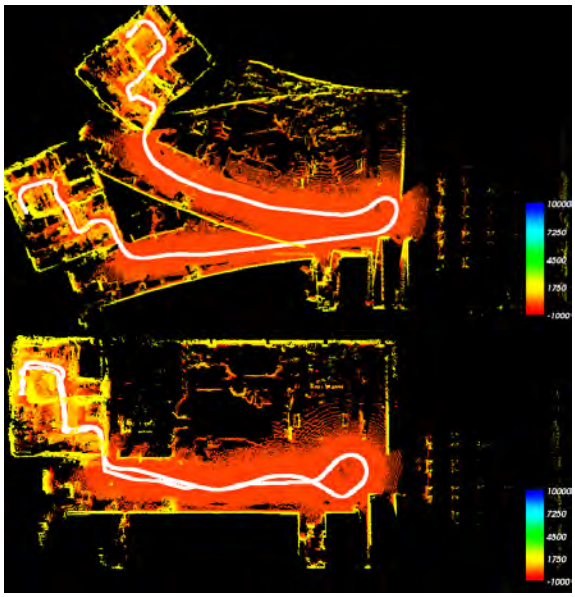

Fig. 1. Odometry tracks of ordinary implementation and gyro-assisted implementation

High-frequency analog noise and rounding errors are handled by averaging multiple samples. The ADC rounding error can be reduced by using the dithering effect for analog noise. In addition, using two complementary gyros attached to the same yaw axis reduces rounding and linearity errors.

Fig.1 shows the tracks of remote-controlled robot(white lines) determined by encoders on wheels, and by gyroscope to measure angular velocity. Each figure shows the results of independent trials where the robot drives uneven curved path in a large room (70[m]$\times$30[m]). The red and yellow dots in the figure represent the measurements from a 2D laser scanner mounted on the robot and aimed at the floor in front of the robot, along with the odometry tracks; these are used to generate a map to compare the results of the two independent trials. The colors of the dots represent their height. The red dots are on the floor and yellow dots are on the walls. The ordinary odometry had large errors, and the start and goal points had an extreme mismatch. As a result, the map showed large strain and deviation. The general distortion may be due to inaccurate parameters for the wheel diameter and tread width. In addition, there may be some local distortion caused by large orientation errors from slippage and bumps when running over cables. In contrast, the results for the gyro-assisted odometry showed very small distortion.

III. Wide view 3D scanner

A. Roundly-swinging laser scanner

To enhance the field of view for the 2D laser scanner, we use a roundly swinging mechanism [11]. A 2D laser scanner attached onto a gimbal, and it is swung by a single actuator to achieve a wide angle of view. Fig. 2 shows a single cycle of the mechanism. The swinging motion extends vertical view angle on every horizontal direction evenly, as a result, whole horizontal view angle of a 2D laser scanner which is 275[°],

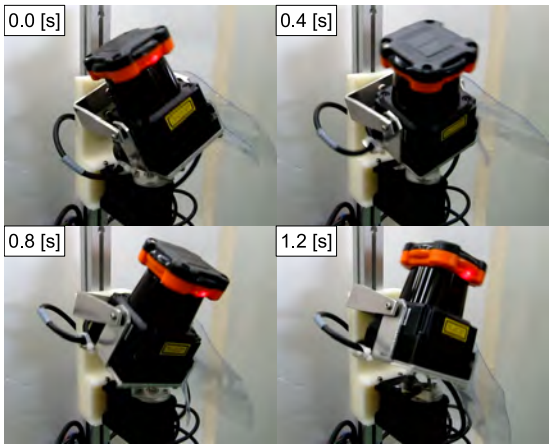

Fig. 2. 3D Scanner

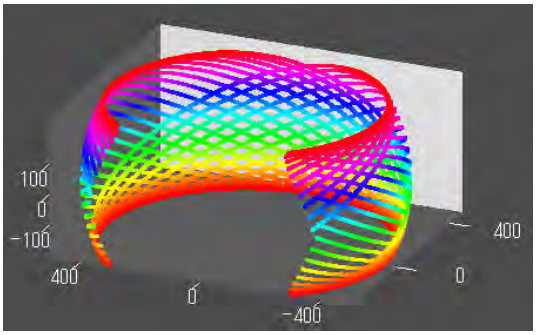

Fig. 3. Simulated FoV of our scanner covering 5/6 of secondary rotation range in 30 scans.

will have the same extended vertical view angle. When the 2D scanner has a view angle of 360[°], this mechanism has a field of view almost equivalent to a scanner with a tilted 2D scanner fixed on a rotating mechanism. This type of 3D scanner has an advantage because of the uniform distribution of measuring points [12].

The roll and pitch angles of the gimbal swing are ± 28[°], so the vertical view angle of the mechanism is ± 28[°]. Fig.3 shows a simulated field of view for the roundly swinging 3D scanner. In all cases, the 2D scanner measured a range of 500 and the swinging actuator moved about 300 [°] by 10 [°] steps. The advantages of this scanner are as follows:

1) The total range of the horizontal view angle has the same extended vertical view angle.
2) The measuring points are uniformly distributed.
3) The actuator is simply controlled since it just rotates at a constant speed.
4) No special cable handling such as slip rings are needed.

Moving the 2D laser scanner in a rotating or nodding manner is a popular method for extending the field of view in 3D. Our roundly swinging scanner is better than the rotating method for points 1, 2 and 4 and is better than the nodding method for point 1-3.

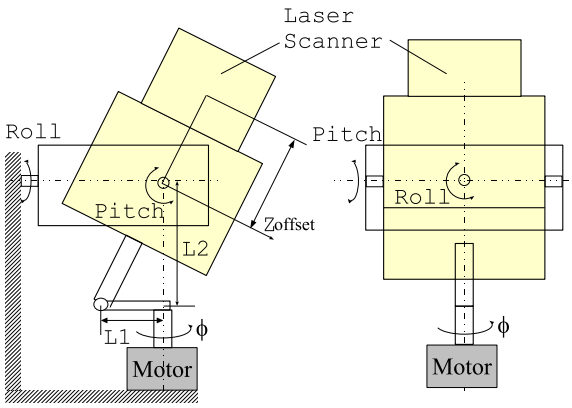

Fig. 4. Scanner structure

B. Calculation of measured point position in 3D

By considering the estimated robot position, sensor position on the robot, posture of the gimbal, 2D laser scanner position on the gimbal and direction of the laser beam, the 3D measurement position can be calculated by applying these transformations in order. The posture of the gimbal can be calculated using the next formula from output link angle ϕ of the swinging actuator and link parameters L_1 and L_2 (Fig.4).

$$Roll(\phi) = \tan^{-1}\frac{y(\phi)}{L_2} \quad (1)$$

$$Pitch(\phi) = \tan^{-1}\frac{x(\phi)}{\sqrt{y^2(\phi)+L_2^2}} \quad (2)$$

where x,y are

$$x(\phi) = L_1\cos\phi \quad (3)$$

$$y(\phi) = L_1\sin\phi \quad (4)$$

The positions of the measured points on the scanner frame are given by

$$P(l,\theta,\phi) = R_x(Roll(\phi))R_y(Pitch(\phi))R_z(\theta)(r,0,z_{offset})^T \quad (5)$$

where θ is the direction of the laser beam, r is the measured distance, z_{offset} is the length between the gimbal rotation center and laser beam window of the 2D laser scanner, and R_x, R_y, R_z are matrices of rotation around the X, Y, and Z axes, respectively. Finally, the point in the global coordinate frame can be calculated by transforming the resulting P using the scanner position on the robot and the robot position estimated with gyro-assisted odometry.

The posture of the gimbal is continuously changing while the laser scanner is scanning, and so the angle ϕ needs to be updated for each θ. In addition, the position and orientation of the robot change continuously, and so these should also be updated for each θ. However, even if the same robot position and orientation are used for the duration of a scan, a resulting point cloud will not be distorted much because the the rotational speed of the robot is relatively slow. As a single ϕ value which is synchronized with θ can be measured for every scan in our method, ϕ value corresponding to each θ

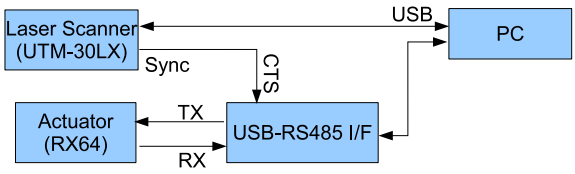

Fig. 5. Sensor block diagram of data flow

can be calculated by interpolating measured ϕ using rotating speed of the swinging actuator.

C. Implementation of the swinging mechanism

The hardware consists of a small-sized 2D laser scanner (HOKUYO UTM-30LX), a smart actuator (ROBOTIS RX-64) to swing the gimbal, and a single board computer to control them. The software consists of three processes — obtaining scans, controlling the actuator and synchronizing data. In our implementation, all the processes run on a single PC. This is an advantage over another implementation [13], which requires a dedicated micro-controller for managing the swinging actuator.

The positions of 3D points can be calculated by using range data from the 2D laser scanner, the posture of the gimbal and the estimated robot position. Synchronizing these three kinds of data is the key to obtaining point clouds without distortion. We use the SYNC signal from the 2D laser scanner to control the outgoing data packet to the smart actuator requesting a report on its output angle (Fig.5). The SYNC signal from the 2D laser scanner triggers data acquisition from the smart actuator, which then triggers data acquisition for odometry on the PC. This simple implementation can synchronize the three types of data more precisely than a method using the time-stamp of each data. In addition, there is no need to monitor the odometry and gimbal posture.

Fig.6 shows a point cloud obtained from the 3D scanner on a moving mobile robot in an outdoor environment. The points on the figure are color-coded by height. In this experiment, the scanning period of the 3D scanner was set to 1.8 [s], and the scanner measured a total of 60 2D scans in a single period. In Fig.6, there are 13 periods of measured points. Although the 2D laser scanner UTM-30LX has a view angle of 270 [°], we limited this to 180[°] because the rear view angle was occluded by the mobile robot itself.

IV. Localization

Self-localization is performed by fusing the position estimated from the gyro-assisted odometry and the measured points of the 3D scanner using a particle filter. A motion model is calculated by measurements from the gyro-assisted odometry, and the robot position is updated within 20 [ms]. The likelihood for the measurement model is calculated by matching an environmental map to measurements of the 3D scanner, for each period (1.8 [s]).

One issue is the computational complexity of matching 3D points from the 3D scanner and an environmental map in 3D. Since the map-matching process is performed for each

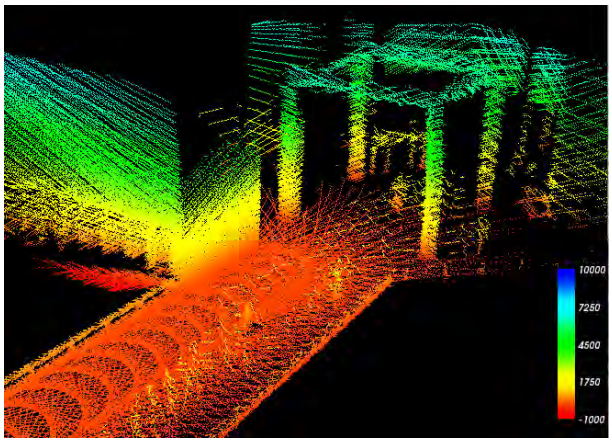

Fig. 6. Example of point cloud captured in outdoor environment

particle, the computational time increases proportionally to the number of particles. This makes the particle filter not work in real-time. To mitigate this problem, we perform the map-matching in 2D using a 2D grid map which summarizes a 3D point cloud. First, a local 2D grid map is generated by projecting a 3D point cloud on to the ground for every 3D scanning period. This local 2D grid map is used to calculate the likelihood of each particle by matching it to a reference 2D grid map generated from a 3D environmental map in advance. This makes the particle filter computationally inexpensive while maintaining the rich information from the wide angle of view.

A reference 2D grid map is generated from 3D points that are collected by a mobile robot with a remote controller from the target environment. The 3D points are then projected into 2D grid cells. The reference 2D map is divided into multiple sub-maps with some overlapping regions to handle large environments. When projecting 3D points into 2D grid cells, to prevent points on the ground or ceiling from being projected, points with specific heights are filtered out. In experiments, we used all points above 15 [cm] and below 45 [cm] for outdoor environments. For indoor environments, an additional filter condition for the ceiling (lower than 2 [m]) was also applied.

Localization with a particle filter sometimes induces a kidnapped state in which no particle is around its correct position on the map. This state is caused by large errors in the motion model or a long time lapse without the effective measurement of environmental features. The kidnapped state is detected by checking if the likelihoods of all particles are lower than a threshold for a certain period of time. When it is detected, particles are redistributed over a wider area to recover the localization failure.

V. Field Experiment

Experiments on autonomous outdoor navigation were conducted at the Tsukuba Challenge. The wheeled mobile robot Papyrus-II was equipped with the proposed system. Fig.7 shows the Papyrus-II robot.

Fig. 7. Mobile robot 'Papyrus II'

A. Tsukuba Challenge

The Tsukuba Challenge is a challenge for outdoor navigation by autonomous mobile robots that takes place on a public street in Tsukuba City, Japan. The task of the challenge is to navigate through a specified course autonomously. Each robot runs accompanied by a judge to check if the task is properly accomplished. In 2009, 72 teams entered the challenge, and five, including us, were successfully accomplished the task. We used the proposed sensor platform; a minimum sensor system with only gyro-assisted odometry and a 3D laser scanner.

Fig.8 shows the environment for 2009. The course was 1.1 [km] long, including a park road and a pedestrian pathway along a street. In addition, the course had a number of difficulties, such as narrow gates, pedestrians, covered area with trees and open spaces that has few features, as shown in Fig. 9. There were a number of buildings and trees near the course, and using GPS in such an environment would cause considerable errors. Laser scanners also do not capture many environmental features in some parts of the course. Moreover, people are passing through the environment going about their lives even while the robot is performing the task.

B. Experiments

Because the task was to navigate through the specified course autonomously, we drove the robot by using an operator to generate an environmental map in advance and then edited the target track by hand on the map. First, an operator steered the robot by driving along the specified course and captured environmental structures along the way with the 3D scanner. All 3D points were arranged using the position estimated with the gyro-assisted odometry, and the reference grid map was generated. The reference grid map was divided into fifteen overlapping sub-maps since the length of the course was 1.1[km]. While referring to the trajectory of the robot as it was steered by the operator, the way points of the target track were then edited by hand.

Fig.10 shows all reference grid maps merged together. The black dots are cells filled with 3D points that passed through the height filter, which was above 15[cm] or below -45 [cm]. The red line shows the target track. As shown in the figure,

Fig. 8. Course of Tsukuba Challenge 2009

Fig. 9. Start position and some difficult areas.

the distortion of the map was very small since estimating the position by the gyro-assisted odometry is sufficiently accurate. The region next to the start point had some overlaps with the region just before the goal area, and the 3D scanner measured some objects twice. By using the position of the corner on a wall in this region, the accumulated errors of the gyro-assisted odometry after traveling 1 [km] can be measured; it was 3.7 [m].

Since the environment is open to public, there were many people walking or cycling through. Moreover, some unexpected objects may appear on the target track. Therefore, we implemented some functions to avoid these obstacles during the experiments. When an unexpected object is detected on the track, the robot slows down its running speed depending

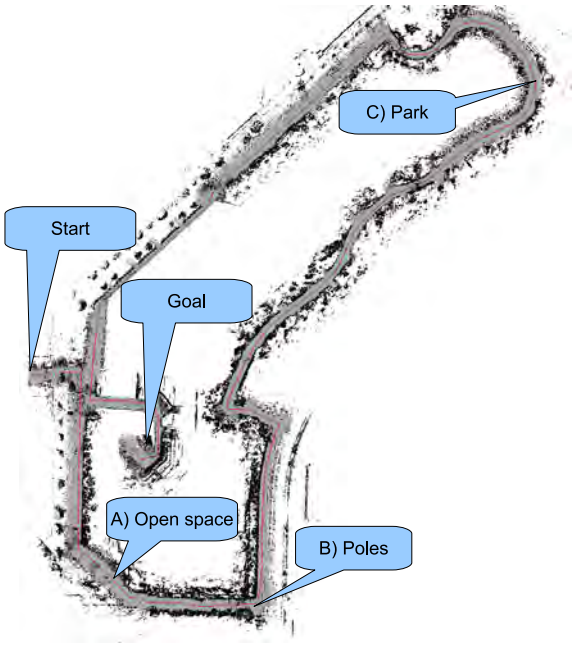

Fig. 10. Generated environment map

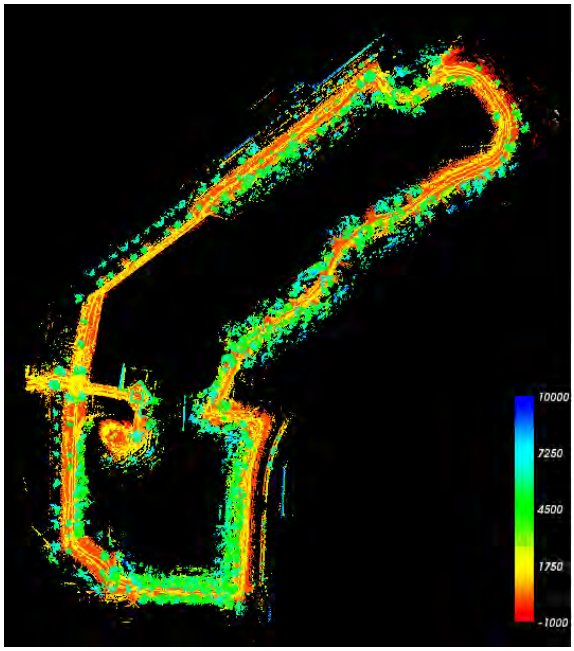

Fig. 11. Collected point cloud during navigation on November 21, 2009

on its distance to the object. If the object does not move away, the robot stops in front of the object. When the robot is blocked by the object for a certain amount of time, the robot plans a new short-term track and avoids the object using the A* algorithm on the local 2D grid map.

C. Results

On November 15, 2009, we ran the robot with an operator to generate a reference grid map and created way points along the target track. Using this map, we conducted navigation experiments six times from November 18 to 21. The results showed the experiments were successful. For all six trials, the robot successfully navigated the 1.1 [km] course autonomously.

Fig.11 shows the result for one experiment on November 20. It shows a point cloud generated by just placing 3D points from the 3D scanner at the positions obtained by the gyro-assisted odometry. Note that no localization scheme was applied in this process. It is slightly distorted, but when compared with Fig. 10, the overall shapes of these two are almost identical. This proves that our gyro-assisted odometry can provide reproducible accuracy. The accumulated errors of the gyro-assisted odometry after traveling 1 [km] was 10.7[m] in this trial. The error is a little larger than that shown in Fig.10, but it still had very high accuracy.

The self-localization system successfully localized the robot position on the reference grid map using the map shown in Fig. 10. Measurements were acquired during runtime, as shown in Fig. 11, and the robot successfully navigated 1.1 [km] in a fully autonomous manner. In the navigation, the robot went through difficult areas including A, B and C shown in Fig. 9.

Point A is an open space where few objects can be observed by 2D laser scanners. Even in such an environment, the 3D scanner was able to acquire many 3D points. Fig. 12 shows two types of local grid maps generated around point A. The left is the actual grid map generated by the 3D scanner, and the right is a grid map generated by a horizontal 2D scanner that was simulated by using the 1-1.5 [m] height slice from the same 3D point cloud. The blue triangle shows the robot position. The figure clearly shows that the horizontal 2D scanner could not obtain enough information while the 3D scanner could. The results indicate that our system can process the particle filter efficiently by using 2D grid maps in map-matching while maintaining much of the information from the wide vertical view of the 3D scanner.

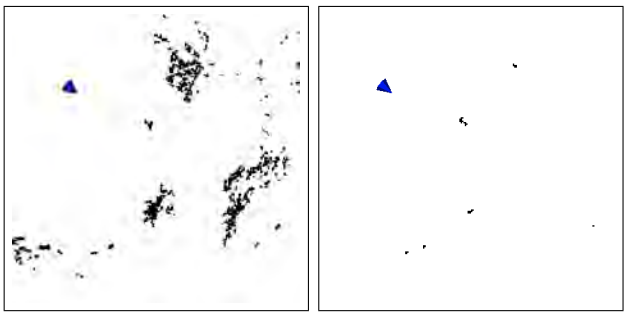

Fig. 12. Point cloud from 3D scanner and simulated 2D scanner at point A

At point B, there were three poles aligned with clearance of 1.5 [m] that required accurate positioning. At this point, rich information could be obtained from the 3D scanner, as shown in Fig. 13. This made the localization results sufficiently accurate, and the robot went between the poles without collisions.

Point C has few features, similar to point A; the lo-

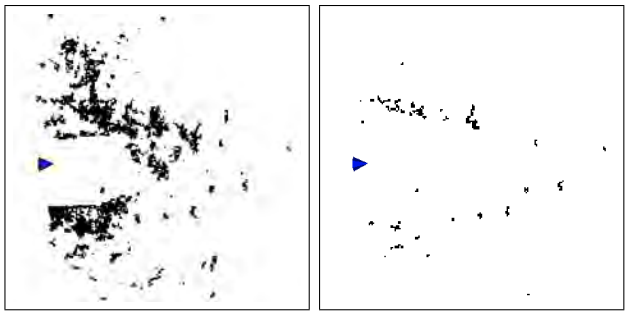

Fig. 13. Point cloud from 3D scanner and simulated 2D scanner at point B

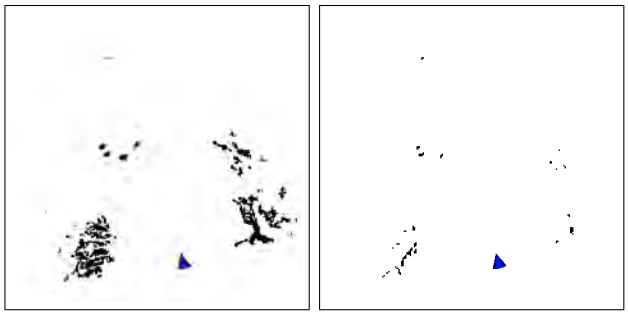

Fig. 14. Point cloud from 3D scanner and simulated 2D scanner at point C

calization system provided enough positioning accuracy to continue the task despite the lack of objects (Fig. 14) due to precise odometry.

Several times in the experiments, a human or other robots happened to block the track. The local path planner using the same 3D scanner as the localization system successfully avoided collision in all the cases.

VI. Conclusion

This paper has proposed a sensor platform for mobile robots that integrates gyro-assisted odometry and a roundly-swinging 3D laser scanner. The gyro-assisted odometry provides highly accurate positioning by dead-reckoning. The 3D laser scanner has a wide field of view and uniform measuring-point distribution. In addition, we implemented a self-localization system using a particle filter with the sensor platform. The self-localization system uses 2D grid maps which are generated by projecting 3D points. The 2D map contains rich information from the wide-view 3D scanner while it has a small data structure. This makes the particle filter computationally inexpensive and provides a robust and lightweight localization system. The reliability and usability of our system was verified through multiple experiments at the Tsukuba Challenge.

Future work includes enhancing the scanning speed and widening the field of view of the 3D laser scanner for higher speed navigation.

References

[1] O. Matsumoto, K. Komoriya, T. Hatase, and H. Nishimura, "Autonomous traveling control of the "tao aicle" intelligent wheelchair," in *Proceedings of the 2006 IEEE/RSJ International Conference on Intelligent Robots and Systems*, pp. 4322–4327, Oct 2006.

[2] K. Iwatsuka, K. Yamamoto, and K. Kato, "Development of a guide dog system for the blind people with character recognition ability," *Pattern Recognition, International Conference on*, vol. 1, pp. 453–456, 2004.

[3] Y. Shimosasa, J. Kanemoto, K. Hakamada, H. Horii, T. Ariki, Y. Sugawara, F. Kojio, A. Kimura, and S. Yuta, "Security service system using autonomous mobile robot," in *Proceedings of the 1999 IEEE International Conference on Systems,Man,and Cybernetics*, vol. 4, pp. 825–829, Oct 1999.

[4] DARPA, "Urban challenge." http://www.darpa.mil/grandchallenge/.

[5] J. J. Leonard and H. F. Durrant-Whyte, "Mobile robot localization by tracking geometric beacons," *Robotics and Automation, IEEE Transactions on*, vol. 7, pp. 376 –382, jun 1991.

[6] S. Thrun, W. Burgard, and D. Fox, *Probabilistic Robotics(Intelligent Robotics and Autonomous Agents)*. The MIT Press, 2005.

[7] B. Barshan and H. F. Durrant-Whyte, "Inertial navigation systems for mobile robots.," *Robotics and Automation, IEEE Transactions on*, vol. 11, pp. 328–342, Jun 1995.

[8] J. Borenstein and L. Feng, "Gyrodometry: A new method for combining data from gyros and odometry in mobile robots," in *Proceedings of the 1996 IEEE International Conference on Robotics and Automation*, (Minneapolis), pp. 423–428, April 1996.

[9] J. Borenstein and L. Ojeda, "Heuristic reduction of gyro drift in gyro-based vehicle tracking," in *SPIE Defense, Security + Sensing; Conference 7305: Sensors, and Command, Control, Communications, and Intelligent (C3I) Technologies for Homeland Security and Homeland Defense VIII*, (Orlando), April 2009.

[10] New Technology Foundation, "Tsukuba challenge: Real world robot challenge." http://www.ntf.or.jp/challenge/. (In Japanese).

[11] Hokuyo Automatic Co., T. Mori, N. Shimaji, S. Yuta, A. Ohya, E. Koyanagi, and T. Yoshida, "Three-dimensional rangefinding device." Japanese Patent Disclosure JP 2008-134163A, 2008.

[12] A. Desai and D. Huber, "Objective evaluation of scanning ladar configurations for mobile robots," in *Proceedings of the IEEE/RSJ International Conference on Intelligent Robots and Systems (IROS)*, October 2009.

[13] M. Matsumoto and S. Yuta, "3d sokuiki sensor module by roundly swinging mechanism and scip-3d interface," in *Proceedings of The 6th International Conference on Ubiquitous Robots and Ambient Intelligence*, (Kimdaejung Convention Center), pp. 37–41, October 2009.